

V. Chabbert
D. Carrie
M. Bennaceur
E. Maupas
V. Lauwers
M. Mhem
T. Lhermusier
M. Elbaz
F. Joffre
H. Rousseau
J. Puel

Evaluation of in-stent restenosis in proximal coronary arteries with multidetector computed tomography (MDCT)

Received: 28 March 2006
Revised: 20 September 2006
Accepted: 12 October 2006
Published online: 18 November 2006
© Springer-Verlag 2006

V. Chabbert (✉) · M. Bennaceur ·
F. Joffre · H. Rousseau
Department of Radiology,
CHU Rangueil,
1 avenue Jean-Poulhes TSA 50032,
31059 Toulouse Cedex 9, France
e-mail: Chabbert.v@chu-toulouse.fr
Tel.: +33-56132-2881
Fax: +33-56132-2492

D. Carrie · E. Maupas · M. Mhem ·
T. Lhermusier · M. Elbaz · J. Puel
Department of Cardiology,
CHU Rangueil,
Toulouse, France

V. Lauwers
Department of Epidemiology,
CHU Rangueil,
Toulouse, France

Abstract The purpose of this study was to assess the ability of 16-slice computed tomography (CT) to detect in-stent restenosis of proximal coronary arteries. From November 2002 to April 2004, 134 consecutive patients with proximal stents (3.25 ± 0.47 mm) were prospectively studied. Multidetector CT (MDCT) was performed 24 h (baseline) and 6 months after angioplasty and analysed by two radiologists blinded to the results of the coronary angiography. Sensitivity, specificity, positive and negative predictive values for in-stent restenosis were compared with conventional quantitative coronary angiography (QCA). Stenosis with a diameter $\geq 50\%$ was considered diagnostic of in-stent restenosis. The CT analysis was performed in 131 and 114 patients at baseline and 6 months, respectively.

The in-stent lumen was evaluable in 111 (121 stents) and 99 patients (108 stents) at baseline and 6 months, respectively. The prevalence of in-stent restenosis was 22.5%. Restenoses were correctly identified in 91.7 and 87.5% by the two radiologists. The sensitivity, specificity, positive and negative predictive values for the assessment of significant in-stent restenosis were 92, 67, 43, 97% and 87, 66, 41, 95% for the radiologists, respectively. MDCT is a potential non-invasive technique for the screening of in-stent restenosis of proximal coronary arteries that needs further improvements.

Keywords Multidetector computed tomography · Coronary stents · Coronary angiography

Introduction

The risk of in-stent restenosis or occlusion in the left main coronary artery (LMCA) or ostial major coronaries (4–30%) may have major clinical consequences and justify an accurate evaluation during follow-up in order to detect the process that could lead to a serious or even fatal complication [1]. So far, only coronary angiography is accepted for the diagnosis of in-stent restenosis. The recent technical developments in multidetector computed tomography (MDCT), with retrospective ECG-gated image reconstruction, have dramatically improved image quality, and MDCT could represent a non-invasive alternative to conventional coronary angiography [2].

Few authors have studied the potential role of MDCT in the detection of in-stent stenosis [3–6], but 4-MDCT could not be considered as a reliable evaluation of in-stent stenosis [5]. Gilard et al. [7] described a sensitivity of 100% and a specificity of 93% with 16-MDCT in a small cohort of 29 patients. On the other hand, Cademartiri et al. [8] showed lower accuracy using 16-MDCT with a sensitivity of 50% and a negative predictive value of 89% for detection of in-stent restenosis and occlusion, although the accuracy was high for detection of stent occlusion only (sensitivity and negative predictive value of 80 and 98%, respectively).

The aim of our study was to evaluate the potential role of 16-MDCT in the detection of in-stent restenosis in

proximal coronary arteries (e.g. the left main or ostial location).

Materials and methods

Patients

One hundred and thirty-four patients were studied prospectively from November 2002 to April 2004 (102 male, 32 female, mean age: 67.4 ± 10.9 years). Patient characteristics are summarized in Table 1. They were eligible to participate if they had at $\geq 50\%$ in the LMCA or $\geq 70\%$ in the ostial coronary artery that was suitable for stent implantation. Patients were enrolled consecutively after stent implantation in the left main (53.73%) or ostial (46.27%) coronary arteries. In the 134 patients, a total of 145 stents (3.25 ± 0.47 mm) were implanted. Lesions

underwent balloon predilation, rotational atherectomy or intravascular ultrasound evaluation, according to the operator's discretion. All the procedures were performed according to standard clinical practice with the same slotted-tube Express bare metal stent (Boston Scientific Corporation, Minneapolis, MN, USA) and the strut thickness was 0.133 mm. Stent locations are listed in Table 2. Patients underwent 16-MDCT 2.5 ± 1.5 days after angioplasty, and both conventional coronary angiography and MDCT at the 6-month follow-up. Exclusion criteria were arrhythmias, intolerance to iodine contrast and renal insufficiency (serum creatinine > 140 mmol/l). The study protocol was approved by the Institution's Ethics Committee and was carried out according to the principles of the Declaration of Helsinki. All of the patients gave a signed informed consent and a grant from the National Research was obtained for this ongoing clinical trial.

Table 1 Patient characteristics. *MI* myocardial infarction

	<i>n</i>	%
Total number of patients	134	100.0
Male	102	76.1
Female	32	23.9
Age	67.4 ± 10.9 (range: 37–86)	
Cardiac risk factors		
Hypertension	76	56.7
Cigarette use	80	59.7
Hyperlipidemia	91	67.9
Diabetes mellitus	32	23.9
Family history	44	32.8
Body mass index (kg/m^2)	25.9 ± 3.5	
Previous coronaropathy	72	53.7
MI	24	17.9
Angina	48	35.8
Previous coronary treatment		
Angioplasty	40	29.8
Coronary bypass	12	9.0
Both (angioplasty+bypass)	4	3.0
None	78	58.2
Coronary status		
1-vessel disease	40	29.9
2-vessel disease	55	41.0
3-vessel disease	39	29.1
Ejection fraction		55.6 ± 11.2
Clinical presentation before stenting (M0)		
Acute MI	35	26.1
Unstable angina	55	41.1
Stable angina	27	20.1
Asymptomatic	17	12.7

Cardiac CT protocol

Data acquisition

CT angiography was performed using a 16-slice MDCT (Sensation 16, Siemens, Forchheim, Germany). The scan parameters were chosen as follows: 16×0.75 mm collimation, table feed of 3.4 mm per rotation, tube rotation time 420 ms, tube voltage 120 kV, reference tube current-time product mAs_{eff} of 530 with the tube modulation program "CareDose 4D". The data were reconstructed applying an effective slice thickness of 0.75 mm with a reconstruction increment of 0.3 mm. All datasets were reconstructed using a field of view of 250×250 mm with a 512^2 reconstruction matrix and a medium smooth body (B30f) convolution kernel. A sharp (B46) convolution kernel was used only in cases of doubt after the analysis of the best phases with the smooth convolution kernel. Nonionic contrast material (90 ml) was injected into an

Table 2 Stent locations

	<i>n</i>	%
Left main	83	57.2
Ostial left main	16	
LM body	4	
LM-LCX ostium	33	
LM-LAD ostium	20	
LM-LCX ostium-LAD ostium (2 "Y" stents)	8	
LM-LCX ostium-MB ostium (2 "T" stents)	2	
LAD ostium	36	24.8
LCX ostium	10	6.9
RCA ostium	15	10.3
Total	145	100

antecubital vein, with a flow rate of 4 ml/s (Iomeron 400, Bracco-Byk Gulden, Constance, Germany). The arm that was injected was kept along the body during the examination. Automated detection of peak bolus enhancement in the aortic root was used for timing of the bolus, a threshold of 100 HU (Hounsfield units) was chosen for the start of the acquisition. During the acquisition, the electrocardiogram was recorded simultaneously for retrospective gating of the data; the patient was told to breath in and hold his/her breath for 20 s, which corresponded to the duration of the acquisition. Oxygen at a rate of 4l/min was delivered to the patient before and during the acquisition to facilitate apnoea. One hundred and twenty-three patients (91.8%) received oral β -blockers for at least 3 days before the scan (100 mg atenolol) to obtain an heart rate lower than 65 bpm; nine received calcium blockers, one amiodarone, and one no heart blocker treatment as his heart rate was lower than 60 bpm. According to the heart rate of the patient, the temporal resolution varied from 105 to 210 ms as a monosegmental reconstruction algorithm was chosen when cardiac frequencies were less than 70 bpm and

bisegmental algorithm when cardiac frequencies were faster than 70 bpm. To evaluate the stents, seven separate reconstructions covering diastole (from -350 to -650 ms before the next R wave) were obtained. Radiation modulation was applied according the absorption values obtained in the thorax during the acquisition ("CareDose 4D"). Images were transferred to a remote workstation (Leonardo, Siemens, Erlangen, Germany) for post-processing and analysis. For each patient, each radiologist chose the datasets containing no or minimal motion artefacts for further analysis.

Data analysis

Two radiologists, blinded to the results of conventional coronary angiography, evaluated all of the CT scans independently. The time between the CT scan test and its analysis was at least 6 months to avoid bias in the analysis. The baseline CT and the 6-month CT were analysed in a random order independently.

Fig. 1 CT scan semiquantitative classification. From the top to the bottom: grades 0, 1, 2, 3. In grade 3, *=distal occlusion beyond the stent

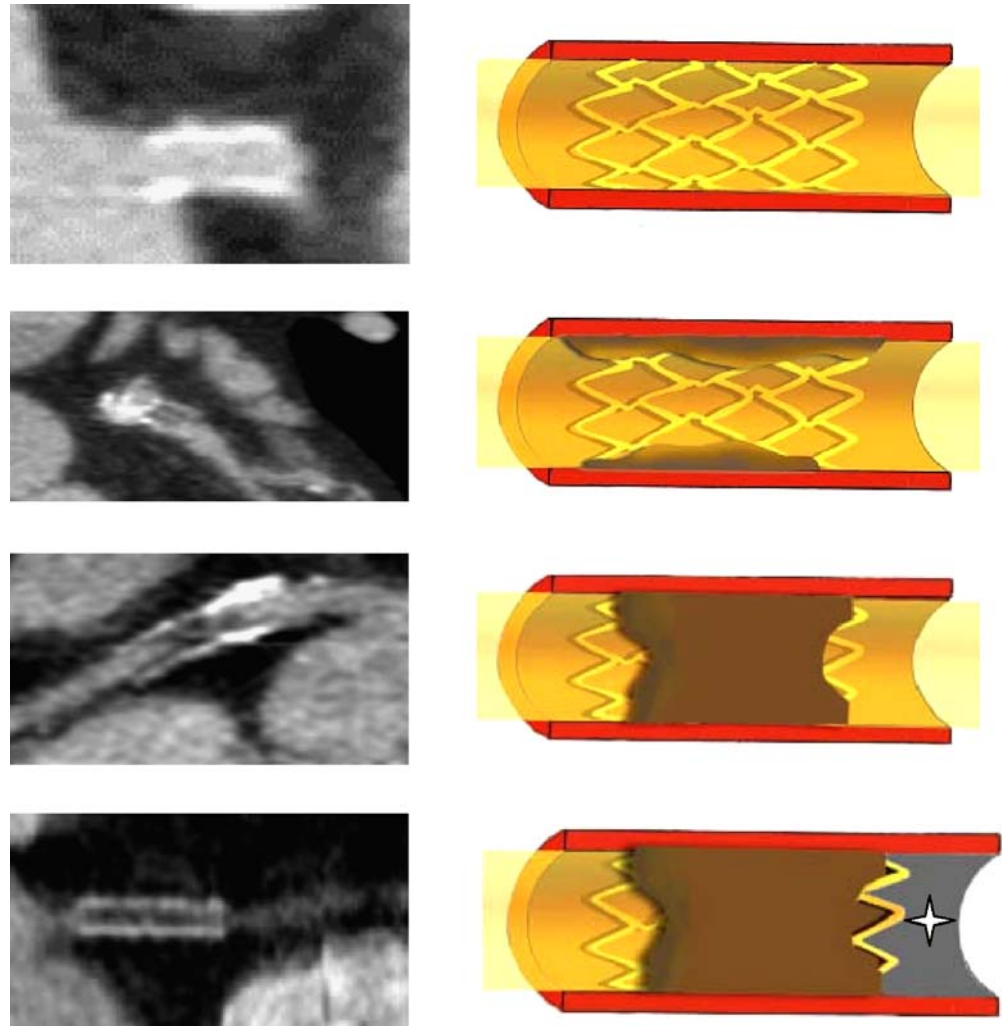


Table 3 Follow-up

Follow-up (6±1.4 months): 120/134 patients (89.55%)	
Clinical follow-up	
Cardiac death: 4 patients (2.98%)	
Global death: 8 patients (5.97%)	
MACE: 27 patients (20.15%)	
Asymptomatic restenosis: 16/32 patients (50%)	
Angiographic data	
Mean reference vessel diameter (before PCI), mm	
Parent branch	3.67±0.52
Side branch (LMCA PCI)	3.03±0.63
Mean stent diameter, mm	3.25±0.47
Angiographic follow-up	
Global restenosis	26.70%
LMCA	22.50%
Restenosis	21.67%
Occlusion	0.83%
Ostial coronary arteries	0.83%

Each time the stent or the coronary vessel could not be analysed correctly (due to stent artefacts, cardiac motion artefacts, poor opacification, small diameter of the stent or the vessel, calcifications), it was graded [4] in the CT scan classification. The original axial images, multiplanar reconstructions (MPR) with double obliquity, curved multiplanar reconstructions were used by the two radiologists for the analysis. Thin-slab maximum intensity projections (MIP) with a slice thickness of 3–5 mm were used for the assessment of the untreated coronary artery segments. The quality of the examination was defined as: (a) good quality when there were no motion artefacts and a good vascular enhancement (with higher enhancement in the aorta than in the pulmonary artery), (b) moderate quality when there were few motion artefacts and/or moderate vascular enhancement (with equivalent enhancement in the aorta and the pulmonary artery or with lower enhancement in the aorta than in the pulmonary artery) and (c) poor quality when the motion artefacts were too numerous and/or vascular enhancement too poor to allow any analysis.

In-stent restenosis was graded according to a five-point semiquantitative classification: (0) no in-stent abnormality,

(1) incomplete in-stent hypodensity with a central contrast enhancement, (2) complete in-stent hypodensity and contrast enhancement beyond the stent, (3) complete in-stent and out-stent hypodensity (representing an in-stent occlusion) and (4) stent non-evaluable (Fig. 1). Grades 1 and 2 corresponded to in-stent stenosis but the spatial resolution of the CT scan could not provide a quantitative analysis. When the stent was classified as non-evaluable, the reasons were listed as follows: motion artefacts, stent artefacts, vascular calcifications, insufficient vascular opacification, vessels too small and respiratory artefacts. In cases of stents located at the ostia of the anterior descending artery or the circumflex artery, the ostium of the non-stented artery, called the side branch, was also assessed according to a four-scale classification: (1) normal diameter or non-significant stenosis (<50% in diameter), (2) significant stenosis (≥50% in diameter), (3) artery occlusion and (4) non-evaluable.

Each time the stent was considered as non-evaluable by one of the two radiologists, a second interpretation by each radiologist was conducted independently with cases chosen at random. The delay between these two interpretations was more than 1 month. The stents which were evaluated with two types of convolution kernel were analysed in consensus by the two radiologists.

Conventional coronary angiography

Data acquisition

In all of the patients, conventional selective coronary angiography was performed using the transfemoral or transradial Judkins approach. Stenting of the left main or the ostial lesions were performed using 6- or 7-French catheters. After stenting, coronary angiography was obtained in two orthogonal views. Coronary angiograms with 6F catheters were performed at 6 months in asymptomatic patients and earlier in those with symptoms.

Data analysis

All angiograms (at baseline and at the 6-month follow-up) were evaluated by two observers in consensus with the use of quantitative coronary angiography (QCA) with auto-

Table 4 Specificity by two radiologists (95% CI: 95% confidence interval)

Specificity at baseline for stents	Radiologist 1	Radiologist 2
Inclusion of NE cases	82.44% (95% CI: 74.83–88.53%)	83.21% (95% CI: 75.68–89.16%)
Exclusion of NE cases	97.30% (95% CI: 92.3–99.44%)	98.20% (95% CI: 93.64–99.78%)
Inclusion of NE cases and second interpretation	85.5% (95% CI: 78.28–91.04%)	86.26% (95% CI: 79.16–91.65%)
Exclusion of NE cases and second interpretation	97.39% (95% CI: 92.56–99.46%)	98.26% (95% CI: 93.86–99.79%)

NE non-evaluable

mated vessel contour detection after catheter-based image calibration (MEDICAL QCA/CMS, MEDIS Imaging System, Leiden, The Netherlands) was used as gold standard for in-stent restenosis detection. The severity of in-stent restenoses was quantified in two orthogonal views. An in-stent lumen diameter narrowing $\geq 50\%$ in diameter (up to in-stent occlusion) was defined as a significant restenosis. The stented vessel was analysed in the same manner as with 16-MDCT: (1) normal diameter or non-significant stenosis ($< 50\%$ in diameter), (2) significant stenosis ($\geq 50\%$ in diameter) and (3) artery occlusion.

Statistical analysis

The kappa statistic was used to estimate interobserver agreement. The thresholds used for interpreting the kappa statistic were below 0.0 poor, 0.0–0.20 slight, 0.21–0.40 fair, 0.41–0.60 moderate, 0.61–0.80 substantial, 0.81–1.00 almost perfect.

We estimated sensitivity, specificity, positive and negative predictive values considering the results of the conventional coronary angiography as the gold standard. Precisions of estimate for diagnostic accuracy were reported with 95% confidence interval (CI) by using exact binomial CI. Statistical analysis was performed using

the Stata software package (StataCorp 2001, Stata Statistical Software Release 7.0, Stata Corporation, College Station, TX, USA).

Results

No patients died in hospital. The 6-month clinical and angiographic follow-up rate was 89.55%. Table 3 shows cardiac events during the follow-up period. A total of eight patients died (5.97%): four of these patients suffered cardiac death. Conventional coronary angiography and MDCT were performed without any complications in all patients.

Conventional coronary angiography

Conventional angiography found a mean reference vessel diameter of 3.67 ± 0.52 mm before PCI (3.03 ± 0.63 mm for side branch distal LMCA). Mean stent diameter was 3.25 ± 0.47 mm.

QCA showed significant left main in-stent restenosis in 27 (22.5%) patients and stent occlusion in 1 (0.83%) patient. The specific location of the restenotic lesions

Table 5 Performances of MDCT for in-stent restenosis by two radiologists^a

Global results at 6 months for stents	Radiologist 1				Radiologist 2			
	Sensitivity	Specificity	PPV	NPP	Sensitivity	Specificity	PPV	NPP
Exclusion of NE cases								
Grade 1	92% (86.5–96%)	67% (58–75%)	43% (34–52%)	97% (88–99%)	87.5% (81–93%)	65.5% (56–74%)	32% (32–50%)	95% (91–99%)
Grade 2	67% (58–75%)	84% (77–91%)	53% (44–62%)	90% (84–96%)	62.5% (53–71%)	86.21% (78–92%)	55.5% (46–65%)	89% (83–95%)
Inclusion of NE cases								
Grade 1	87.5% (81–94%)	72.5% (54–81%)	39% (29–49%)	97% (93–100%)	81% (73–90%)	71% (62–80%)	36% (26–45%)	95% (90–99%)
Grade 2	50% (40–60%)	91% (86–97%)	53% (43–63%)	90% (84–96%)	44% (34–54%)	94% (89–98%)	58% (48–68%)	89% (83–95%)
Second interpretation and exclusion of NE cases								
Grade 1	87.5% (81–93%)	68% (59–76%)	43% (34–52%)	95% (91–99%)	76% (76–90%)	67% (58–75%)	41% (32–50%)	93.5% (89–98%)
Grade 2	58% (49–57%)	85% (78–91%)	52% (42–61%)	88% (82–94%)	54% (49–57%)	87% (81–93%)	54% (45–63%)	87% (81–93%)
Second interpretation and inclusion of NE cases								
Grade 1	85% (78–91%)	71% (62–79%)	42% (32–51%)	95% (91–99%)	80% (72–87%)	70% (61–79%)	39% (30–48%)	93.5% (89–98%)
Grade 2	50% (40–59%)	89% (93–95%)	53% (43–62%)	88% (82–94%)	45% (35–54%)	91% (86–96%)	56% (47–65%)	87% (81–93%)

^aResults with two threshold values in the CT scan classification are shown. The 95% confidence intervals in percentages are presented in parentheses. *NE* non-evaluable, *PPV* positive predictive values, *NPP* negative predictive values

according to the LMCA and ostial coronary artery segments involved are presented in Table 3. The prevalence of diffuse restenosis was 26.7%. Angiographic restenosis was totally asymptomatic in 16 of 32 patients (50%) and was totally independent of the severity of in-stent restenosis. The equivalent effective dose was of 24 mSv per patient and per examination.

Multislice computed tomography

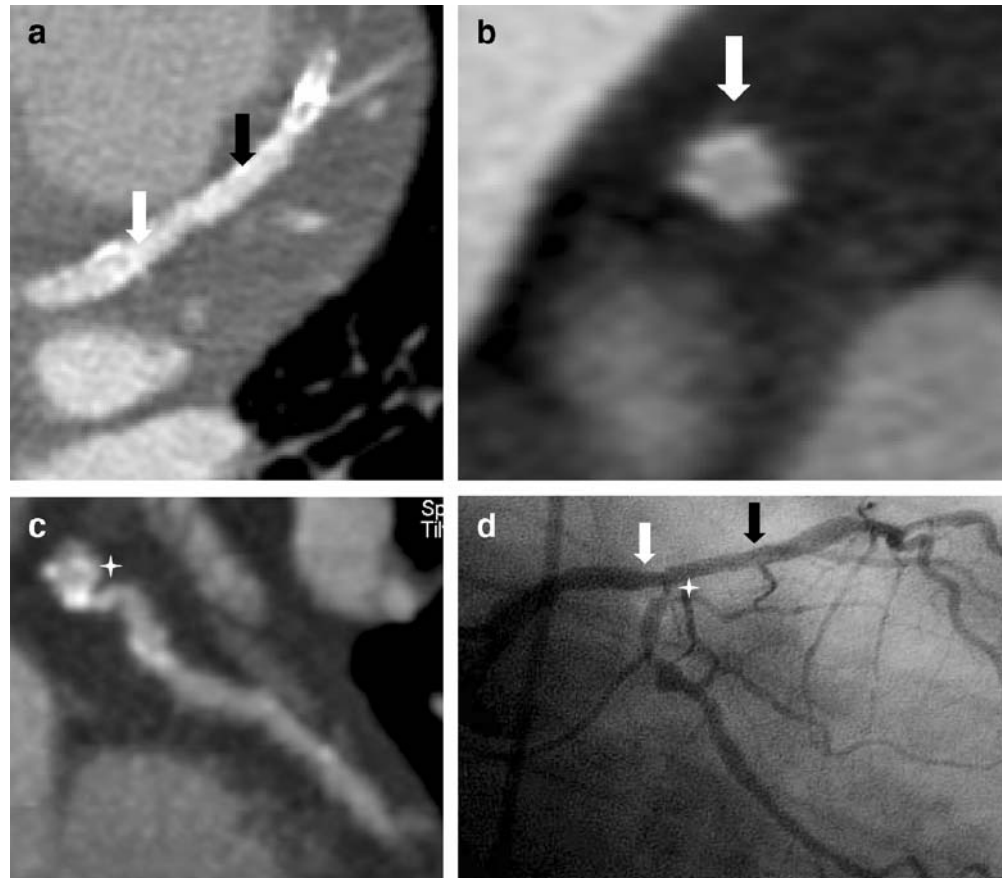
The CT analysis was performed in 131 patients at baseline and 114 patients at the 6-month follow-up. The CT scan analysis could not be done in 3 patients (2%) at baseline (CT scan raw data lost) and in 20 patients (15%) at the 6-month follow-up [7 patients (5.2%) died, 10 patients (7.5%) were lost to follow-up and CT scan raw data were lost for three patients (2%)]. At the 6-month follow-up, the quality of the CT scan was estimated as good in 58.5%, moderate in 43% and poor in 0.9%. The cause of poor quality examinations was a bad vascular enhancement. The heart rate was 53.8 bpm at baseline and 53 bpm at the 6-month follow-up. The equivalent effective dose was of 7.2 ± 1.6 mSv per patient and per examination.

The in-stent lumen was evaluable in 111 of 131 patients (85%) at baseline and in 99 of 114 patients (87%) at 6 months. At baseline, 121 stents were evaluable (one stent/patient in 101 patients and 2 stents/patient in 10 patients). At the 6-month follow-up, 108 stents were evaluable (1 stent/patient in 90 patients and 2 stents/patient in 9 patients).

At baseline, only the specificity could be calculated as there was no in-stent stenosis. Considering a threshold value of grade 1 in the CT scan classification, the specificity was 82 and 83% for the two radiologists with inclusion of the non-analyzable cases (Table 4). The results for the two radiologists after exclusion of the non-analyzable cases and the second interpretation of the non-analyzable cases are summarized in Table 4. The kappa between the two radiologists at baseline was excellent ($k=0.92$).

At 6 months, the prevalence of in-stent restenosis was 22.5% (27 patients) on coronary angiography. Of the 24 analyzable restenoses explored by both techniques, 22 (91.7%) were correctly identified by one of the two radiologists (threshold value grade 1) in the semiquantitative CT scan classification and 21 of 24 restenoses (87.5%) by the other radiologist. The overall results for the two

Fig. 2 Example of a true negative case for the stent (*white arrow*) located in the distal part of the left main artery and the origin of the anterior descending artery. **a** Longitudinal MPR view of the stent and the anterior descending artery. **b** Axial MPR view of the stent. **c** MIP oblique view of the circumflex artery. **d** Right anterior view of the coronary angiography. True positive for the origin of the circumflex artery with a more than 50% stenosis (*star*). True negative for the anterior descending artery beyond the stent where there is no significant stenosis (*black arrow*). Normal in-stent lumen on the CT scan (grade 0) (**a-c**) and on the coronary angiography (**d**)



radiologists, with inclusion or exclusion of the non-evaluable cases and after second interpretation of the non-evaluable cases, are summarized in Table 5 (Figs. 2, 3, 4 and 5). The sensitivity, specificity, positive and negative predictive values for the assessment of significant in-stent

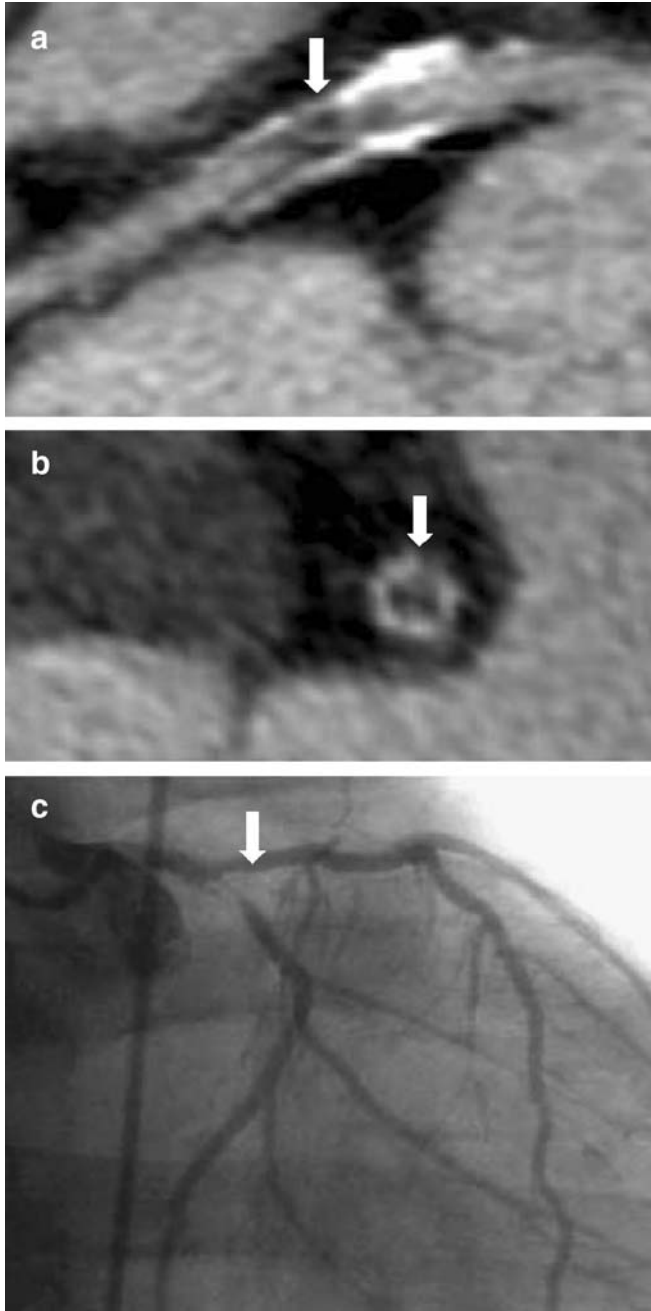


Fig. 3 Example of a true positive for the stent with an in-stent restenosis more than 50% in diameter, classified grade 2 on the CT scan. **a** Longitudinal MPR view of the left main artery, the stent (white arrow) and the circumflex artery beyond the stent. **b** Axial MPR view of the stent. **c** Coronary angiography with a right anterior view

restenosis ($\geq 50\%$) were 92, 67, 43 and 97% for the first radiologist and 87, 66, 41 and 95% for the second radiologist, respectively, when considering the first threshold of abnormality on CT scan (CT scan considered as positive for stenosis from grade 1 to 3 in the CT scan classification) (Table 5). The kappa between the two radiologists for the stents at 6 months was good ($k=0.76$). The results observed when choosing a higher threshold (grade 2, i.e. CT scan considered positive for stenosis from grade 2 to 3 lesions) are summarized in Table 5. As expected, when considering this higher threshold, the performances decreased in terms of sensitivity (67 and 62.5% for the two radiologists, respectively). However, the negative predictive value remained high (90 and 89% for the two radiologists, respectively) (Table 5). Several factors that could influence the classification of the patients were studied: age of the patients (older than 70 years of age), presence of calcifications, diameter of the stents (although the mean stent diameter was 3.25 ± 0.47 mm), heart rate, cardiac phases reconstructed, quality of opacification and examination. None of them was significantly involved in the wrong results (false positives and false negatives).

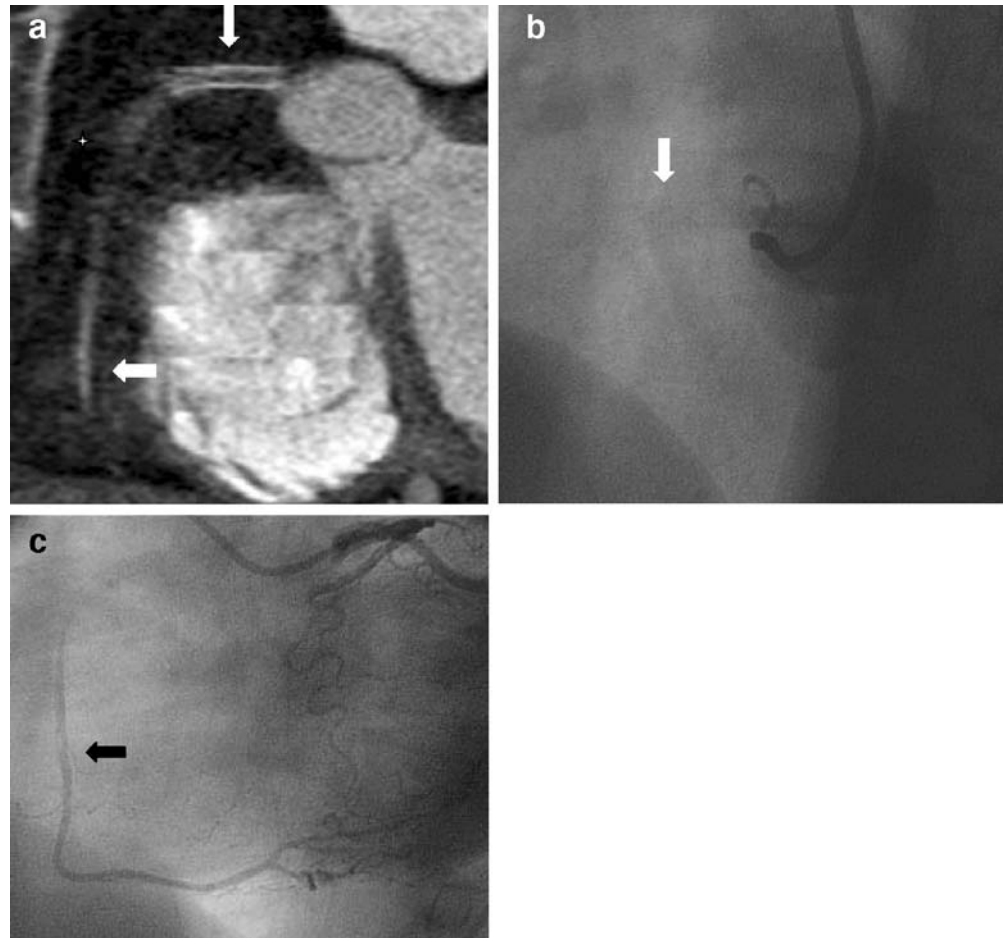
The results for the diagnosis of stenosis in the side branch at 6 months are summarized in Table 6 (Figs. 2, 3, 4 and 5). The sensitivity, specificity, positive and negative predictive values were, respectively, 82, 55, 35 and 91% for the first radiologist and 82, 58, 36 and 92% for the second radiologist [threshold value grade 2 (significant stenosis) in the classification]. The kappa between the two radiologists was excellent ($k=0.9$).

Thirty-three patients (37 stents) were explored with two types of convolution kernel at the 6-month follow-up. Twenty-nine patients had normal stents or non-significant in-stent restenosis and three patients had significant in-stent restenosis on conventional coronary angiography (Table 7). Among the 22 patients with normal stents on coronary angiography, 18 were correctly graded 0 according to the CT scan classification with both convolution kernels: nine were better analysed with the sharp kernel in comparison with the smooth one, eight were equally analysed and one was less well analysed with the sharp one. One patient evaluated grade 1 with the smooth kernel (false positive) was correctly evaluated with the sharp one and one patient of three scored as non-evaluable with the smooth kernel was correctly scored grade 0 with the sharp one. Among the patients with significant in-stent restenosis on coronary angiography, all were correctly scored (grade 2) with the smooth kernel; the results did not change with the sharp convolution kernel.

Discussion

The aim of our study was to evaluate the potential role of 16-MDCT in the detection of in-stent restenosis in proximal coronary arteries.

Fig. 4 Example of a true positive case with an in-stent occlusion. **a** Oblique MPR view of the right coronary artery showing the in-stent occlusion (grade 3) (*white arrow*), occlusion of the second part of the artery, just beyond the stent (*star*) and enhancement of the distal part of the artery from the left coronary arteries (*black arrow*). **b, c** Coronary angiography centered on the right coronary artery showing its occlusion due to the in-stent occlusion (*white arrow*). Injection in the left main artery showing the opacification of the second part of the right coronary artery beyond the stent (*black arrow*)



In-stent restenosis is the main limiting factor for the long-term efficacy of coronary stenting in complex lesions. In cases of left main stenting, restenosis could be associated with increased long-term mortality. Because in-stent restenosis is often asymptomatic (16 of 32 patients in our series), its detection with non-invasive technology is clinically relevant.

To our knowledge, this is the first study that assesses a large number of proximal stents with 16-MDCT. Moreover, all stents belong to the same manufacturer (Express stents, Boston Scientific Corporation, Minneapolis, MN, USA) which provides a homogeneous population. A few authors have studied the potential role of MDCT in the detection of in-stent stenosis and occlusion in vivo in smaller populations [3–7]. Schuijf et al. [4] showed a sensitivity of 78% and a specificity of 100% in a group of 22 patients with 65 stents (14 different stent types) varying from 2.25 to 5 mm in diameter. Gilard et al. [7] described a sensitivity of 100% and a specificity of 93% in a recent study of 29 patients (4 restenoses). Moreover in these studies [3, 4], different types of stents were used, some of which were known to induce more important artefacts on MDCT (Wiktor Hepamed stents, Tristar stents).

We used one type of stent to have a homogeneous study group. This stent is known to give less artefacts on cardiac CT. In this regard, Mahnken et al. [9] insisted on the influence of the material on the visibility of the in-stent lumen on MDCT in vitro: they showed that gold and gold-coated stents caused the most severe artefacts. On the contrary, stents with slim profiles showed fewer artefacts in the group of stainless steel stents. On MDCT images, the stent struts appear larger than they actually are due to partial volume effect. This phenomenon associated with beam hardening results in a higher average CT density value within the stent than outside the stent [10]. By using 64-slice CT, Maintz et al. [11] showed that the majority of stents tested (68 stents) had a lumen visibility of more than 50% of the stent diameter. With three other stents (Pixel, Rithron XR, Sito), the Express stent had a lumen visibility of 50% of the stent diameter and only ten stents had a lumen visibility of less than 50%.

The other factors that favourably influenced the visibility of the in-stent lumen in in vitro studies were: a thinner collimation (16-MDCT provides submillimetric collimation in comparison to 4-MDCT), a sharp kernel algorithm reconstruction and a larger diameter of the stent. Mahnken

Fig. 5 True positive case for the stent with an in-stent restenosis (*white arrow*), classified grade 1 on the CT scan. Concerning the circumflex part of the stent, the origin and the first part of the anterior descending artery appears normal, although the second part appears irregular without significant stenosis (true negative for the collateral) (*star*). The circumflex artery beyond the stent with a 50% stenosis on the CT scan and coronary angiography (*black arrow*). **a** Longitudinal MPR view of the left main artery and the origin of the circumflex artery with the in-stent restenosis (*white arrow*). **b** Longitudinal MPR view of the circumflex artery showing the in-stent stenosis and the artery beyond the stent. **c** Longitudinal MIP view of the anterior descending artery. **d** Left caudal view on coronary angiography

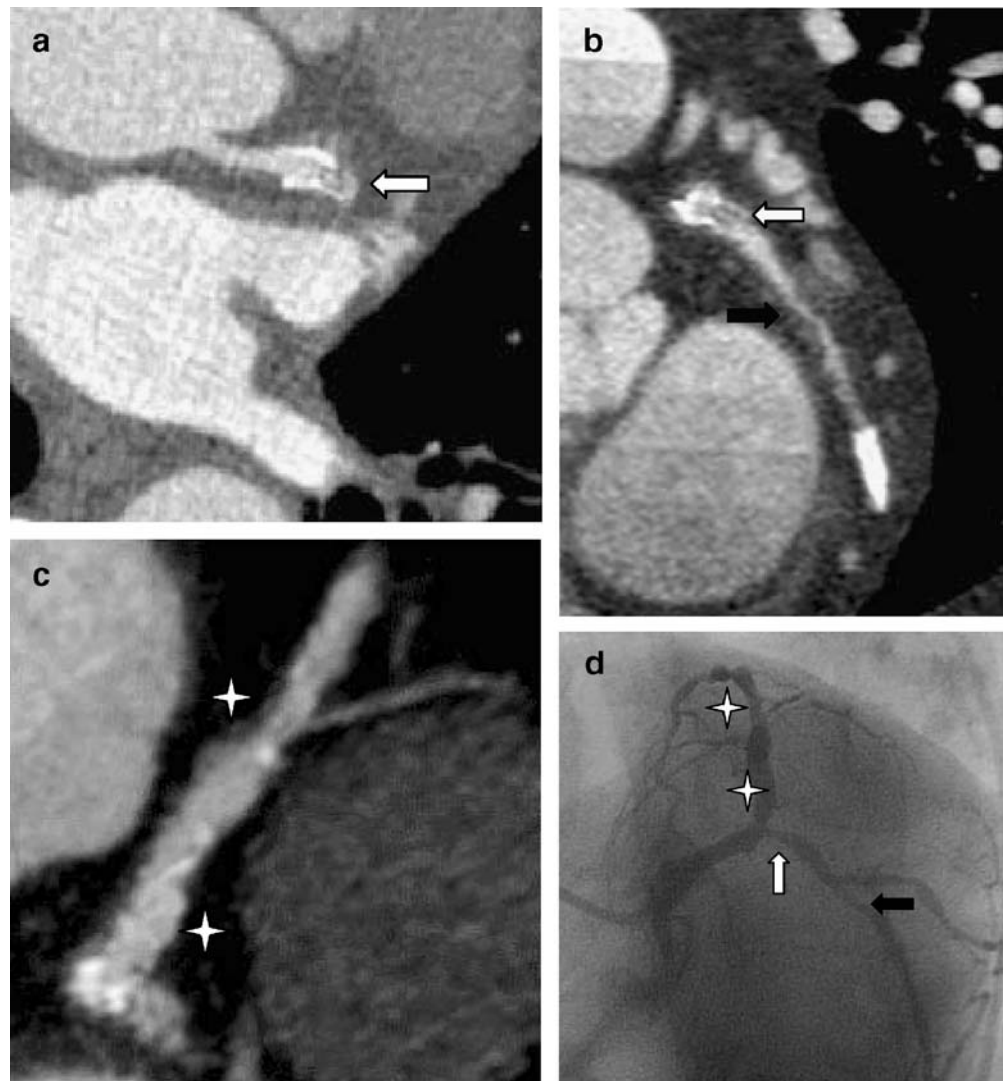


Table 6 Stenosis of side branches by two radiologists^a

Global results at 6 months for side branches	Radiologist 1				Radiologist 2			
	Sensitivity	Specificity	PPV	NPP	Sensitivity	Specificity	PPV	NPP
Inclusion of NE cases	82%	55%	35%	91%	82%	56%	36%	92%
	(71–93%)	(41–69%)	(21–48%)	(83–99%)	(71–93%)	(44–73%)	(22.5–49%)	(84–99%)
Exclusion of NE cases	78%	68%	41%	91%	78%	71%	44%	92%
	(65–91%)	(53–82%)	(26–56%)	(72–99%)	(65–91%)	(57–85%)	(28–59%)	(83–100%)
Second interpretation and inclusion of NE cases	82%	58%	36%	92%	82%	60.5%	37.5%	92%
	(71–93%)	(44–72%)	(23–50%)	(84–99%)	(71–93%)	(47–74%)	(24–51%)	(84–100%)
Second interpretation and exclusion of NE cases	80%	67%	42%	92%	80%	70%	44.5%	92%
	(68–92%)	(53–81%)	(27–57%)	(83–100%)	(68–92%)	(56–83%)	(30–59%)	(84–100%)

^aThe 95% confidence intervals in percentages are presented in parentheses. *NE* non-evaluable, *PPV* positive predictive values, *NPP* negative predictive values

Table 7 Comparison of the two convolution kernels for 33 patients (37 stents)

	Normal stents		< 50% in-stent restenosis		≥ 50% in-stent restenosis	
	Smooth K	Sharp K	Smooth K	Sharp K	Smooth K	Sharp K
GRADES						
According to	0 (18pat)	0 (18 pat - 9 better 8 equally 1 less)	0 (4 pat) [10%,30% 40%]	0 (3 pat - 3 better) 1 (1 pat)	2 (3 pat) [60%,70%, 80%]	2 (3 pat- 3 equally)
Ct-scanner classification	1 (1 pat)	0	1 (1 pat) [10%]	1		
			NE (2 pat) [10%,20%]	NE		
	NE (3 pat)	NE (2 pat) 0 (1 pat)	9 stents in 7 patients: 7 stents with non significant stenosis and 2 normal stents (grade 0 with both kernels, equally analysed).		5 stents in 3 patients: 3 stents with restenosis and 2 normal stents (grade 0 with both kernels, equally analysed)	

K: kernel. The number of patients are presented in parentheses. The percentages represent the quantification of the in-stent restenosis on coronary angiography

et al. [12] compared 64-MDCT and 16-MDCT for the assessment of eight coronary artery stents in a phantom study; by using an effective slice thickness of 0.6 mm with 64-MDCT, 1 mm with 16-MDCT and a reconstruction increment of 0.3 mm in both scanners, the average visible stent lumen was 53.4% using 64-MDCT and 47.5% with 16-MDCT at the expense of an increase in image noise by 30% due to thinner slice thickness. Although the sharp kernel algorithm significantly increased the noise in comparison to the smooth kernel one, it significantly improved the visibility of the in-stent normal lumen and the in-stent stenosis in in vitro studies [11, 13, 14]. We did not systematically apply the sharp convolution kernel, because in most of the cases the stent could be analysed; we used it only in cases of doubt after analysis of the best phases with the smooth kernel. Actually, the noise is increased with the sharp kernel algorithm reconstruction and in our experience, analysis of non-treated coronary segments is generally hampered. Maintz et al. [15] and Seifart et al. [16] have shown that using sharp kernel algorithm reconstruction increased the in-stent lumen visibility, but Seifart et al. [16] showed that it significantly increased the noise too. In our experience, we are in agreement with that: we conducted an in vitro study (not published) at the end of our clinical study, comparing B30 and B46 convolution

kernels with 16-slice CT, with flat panel angiography as the gold standard. The sharp kernel significantly improved the visibility of the normal stent (3 mm in diameter) at the expense of a significant increase in noise but not the diagnosis of restenosis. In our study, 33 patients were studied with the two types of convolution kernel at the 6-month follow-up (3 patients with significant in-stent restenosis, 7 patients with non-significant in-stent restenosis and 22 patients with normal stents). In cases of in-stent significant restenosis the sharp kernel did not change the classification which was already correct with the smooth one. On the other hand, in cases of normal stents, the sharp convolution kernel improved the visibility of the stent (grade unchanged however) in more than half of the patients. It favourably changed the score for only two patients (one non-evaluable case and one false positive case). In cases of non-significant in-stent restenosis (7 patients), the sharp convolution kernel did not change the score except for one patient unfavourably causing a false positive [limit lesion (40%) however]. The only in vivo experiences, comparing these two kernel algorithm reconstructions, are those of Hong et al. [3] and Seifart et al. [16] who demonstrated that the use of the sharp kernel algorithm significantly improved the estimation of in-stent luminal diameter in comparison to the smooth one

(normal stents). As a whole, to date, we do not know the actual impact of this kernel algorithm reconstruction in routine use for the analysis of the native coronary arteries and the in-stent restenosis in patients in comparison to the smooth one. The impact of stent diameter has been discussed by some authors [2, 4]. Schuijf et al. [4] showed that stents less than 3 mm in diameter were more often non-assessable with 16-MDCT than stents more than 3 mm. Moreover, in most experimental studies, the authors tested stents between 3 and 4 mm in diameter [9, 11, 12]. Stents of less than 3 mm in diameter are difficult to analyse with MDCT due to a strong reduction of lumen visibility. In our study, the stents were proximal and they had a diameter of more than 3 mm in almost all cases, which can explain the high proportion of evaluable stents at baseline and follow-up (85 and 87%, respectively).

Our results showed interesting performances in terms of sensitivity and negative predictive values when considering the first threshold value, i.e. from grade 1 to grade 3 in the semiquantitative CT scan classification. Considering a grade 2 threshold value, the performances dropped for the sensitivity although, the negative predictive value remained high. The spatial resolution provided by 16-slice MDCT is still imperfect to allow a precise characterization of in-stent abnormalities compared to coronary angiography, which explains some overlap between grades 1 and 2 lesions on CT scan in our study. This is in agreement with the results of Cademartiri et al. [8] who reported a sensitivity of 50% and a negative predictive value of 88% with a 16-slice MDCT, by choosing a threshold value equivalent to grade 2 in our classification. As demonstrated by other authors, our study shows it is difficult to propose a quantitative evaluation of the in-stent restenosis with 16-slice MDCT. Theoretically, the use of the newest generation MDCT (40 and 64 slices and dual source MDCT) will probably improve the performances due to better spatial and temporal resolutions. Although the results of Gaspart et al. [17] with a 40-slice MDCT are in agreement with ours, not all stents were proximal in their series and obviously there is a need for other studies in this regard. Despite the evolving nature of this technology, it seems important to state the performances of 16-slice MDCT for the assessment of proximal in-stent restenosis in a large population. Even if the improved spatial resolution of 64-MDCT results in superior assessment of coronary stent lumen compared to 16-MDCT, a relevant part of the stent lumen is still not assessable with MDCT [12]. With the newest generation MDCT, we can expect better results in terms of PPV and specificity but NPV and sensitivity probably close to those described with 16-MDCT.

The ostia of the side branches (proximal native arteries abutting on the stented segment) could also be analysed in our population at 6 months with acceptable performances (sensitivity of 82% and negative predictive values of 91–92%). The analysis must not only detect abnormality in the stent, but also in the proximal side branch abutting on the stent, as depiction of significant stenosis at this location can be clinically relevant. Our results concerning these proximal native coronary arteries are in agreement with results already published in the literature concerning native arteries [2, 18, 19]. However, to our knowledge, there are no data available in the literature assessing the effects of stent artefacts on the side branch in terms of performances for stenosis depiction.

Study limitations

The number of patients lost to follow-up is significant but is typical of a population at this age with this type of disease. However, the statistical power of our population provided satisfactory estimation of the 16-MDCT performances in comparison with conventional coronary angiography for the prevalence of in-stent restenosis.

We did not use the sharp kernel algorithm reconstruction in comparison to the smooth one for all of our patients for the reasons already stated. In spite of this limit, our results are encouraging and although the sharp kernel increased the visibility of the normal stents in half of the patients, it did not significantly change the final classification of our group of patients. It could be interesting to study its impact in vivo in comparison to the smooth one for more patients with significant in-stent restenosis. The modulation of radiation during systole (ECG pulsing) was not applied as early (–650 ms) and late (–350 ms) phases during diastole were used for the reconstructions; in cases of high heart rates, the decrease in radiation applied during systole can affect early and late diastole and hamper the analysis.

The recent guidelines emphasise the use of ECG pulsing in routine practice when it is possible (i.e. for low heart rates) to significantly reduce the effective dose to the patient.

In conclusion, 16-slice computed tomography is a potential non-invasive technique with high sensitivity and negative predictive value for the screening of in-stent stenosis of proximal coronary arteries that needs further improvements.

Acknowledgments To Dr. A. Gozlan for the drawings.

References

1. Takagi T, Stankovic G, Finci L et al (2002) Results and long-term predictors of adverse clinical events after elective percutaneous interventions on unprotected left main coronary artery. *Circulation* 106:698–702
2. Schoepf UJ, Becker CR, Ohnesorge BM, Yucel EK (2004) CT of coronary artery disease. *Radiology* 232:18–37
3. Hong C, Chrysant GS, Woodard PK, Bae KT (2004) Coronary artery stent patency assessed with in-stent contrast enhancement measured at multi-detector row CT angiography: initial experience. *Radiology* 233:286–291
4. Schuijf JD, Bax JJ, Jukema JW, Lamb HJ, Warda HMA, Vliegen HW, de Roos A, Van der Wall EE (2004) Feasibility of assessment of coronary stent patency using 16-slice computed tomography. *Am J Cardiol* 94:427–430
5. Ligabue G, Rossi R, Ratti C, Favali M, Modena MG, Romagnoli R (2004) Noninvasive evaluation of coronary artery stents patency after PTCA: role of multislice computed tomography. *Radiol Med (Torino)* 108(1–2):128–137
6. Maintz D, Grude M, Fallenberg EM, Heindel W, Fischbach R (2003) Assessment of coronary arterial stents by multislice-CT angiography. *Acta Radiol* 44:597–603
7. Gilard M, Cornily JC, Rioufol G, Finet G, Pennec PY, Mansourati J, Blanc JJ, Boschat J (2005) Noninvasive assessment of left main coronary stent patency with 16-slice computed tomography. *Am J Cardiol* 95:110–112
8. Cademartiri F, Marano R, Runza G, Mollet N, Nieman K, Luccichenti G, Gualerzi M, Brambilla L, Coruzzi P, Galia M, Midiri M (2005) Non-invasive assessment of coronary stent patency with multislice CT: preliminary experience. *Radiol Med (Torino)* 109(5–6):500–507
9. Mahnken AH, Buecker A, Wildberger JE, Ruebben A, Stanzel S, Vogt F, Günther RW, Blindt R (2003) Coronary artery stents in multislice computed tomography: in vitro artefact evaluation. *Invest Radiol* 39(1):27–33
10. Nieman K, Cademartiri F, Raaijmakers R, Pattinama P, De Feyter P (2003) Noninvasive angiographic evaluation of coronary stents with multi-slice spiral computed tomography. *Herz* 28:136–142
11. Maintz D, Seifarth H, Raupach R, Flohr T, Rink M, Sommer T, Ozgün M, Heindel W, Fischbach R (2006) 64-slice multidetector coronary CT angiography: in vitro evaluation of 68 different stents. *Eur Radiol* 16:818–826
12. Mahnken AH, Muhlenbruck G, Seyfarth H, Flohr T, Stanzel S, Wildberger JE, Gunther KW, Kuettner A (2006) 64-slice computed tomography assessment of coronary artery stents: a phantom study. *Acta Radiol* 47(1):36–42
13. Maintz D, Juergens KU, Wichter T, Grude M, Heindel W, Fischbach R (2003) Imaging artery stents using multislice computed tomography: in vitro evaluation. *Eur Radiol* 13:830–835
14. Mahnken AH, Seyfarth T, Flohr T, Herzog C, Stahl J, Stanzel S, Kuettner A, Wildberger JE, Gunther RW (2005) Flat-panel detector computed tomography for the assessment of coronary artery stents: phantom study in comparison with 16-slice spiral computed tomography. *Invest Radiol* 40(1):8–13
15. Maintz D, Seifarth H, Flohr T, Krämer S, Wichter T, Heindel W, Fischbach R (2003) Improved coronary artery stent visualization and in-stent stenosis detection using 16-slice computed-tomography and dedicated image reconstruction technique. *Invest Radiol* 38:790–795
16. Seifarth H, Raupach R, Schaller S et al (2005) Assessment of coronary artery stents using 16-slice MDCT angiography: evaluation of a dedicated reconstruction kernel and a noise reduction filter. *Eur Radiol* 15(4):721–726
17. Gaspard T, Halon DA, Lewis BS, Adawi S, Schliamser JE, Rubinshtein R, Flugelman MY, Peled N (2005) Diagnosis of coronary in-stent restenosis with multidetector row spiral computed tomography. *J Am Coll Cardiol* 46(8):1573–1579
18. Martuscelli E, Romagnoli A, D'Eliseo A, Razzini C, Tomassini M, Massimiliano S, Simonetti G, Romeo F (2004) Accuracy of thin-slice computed tomography in the detection of coronary stenoses. *Eur Heart J* 25:1043–1048
19. Giesler T, Baum U, Ropers D, Ulzheimer S, Wenkel E, Mennicke M, Bautz W, Kalender WA, Daniel WG, Achenbach S (2002) Noninvasive visualization of coronary arteries using contrast-enhanced multidetector CT: Influence of heart rate on image quality and stenosis detection. *AJR Am J Roentgenol* 179:911–916